Molecular Therapy
Oncolytics
Original Article

Development of a Novel Class of Self-Assembling dsRNA Cancer Therapeutics: A Proof-of-Concept Investigation

Vishwaratn Asthana,[1] Brett S. Stern,[1] Yuqi Tang,[1] Pallavi Bugga,[1] Ang Li,[1] Adam Ferguson,[1] Anantratn Asthana,[1] Gang Bao,[1] and Rebekah A. Drezek[1]

[1]Department of Bioengineering, Rice University, Houston, TX 77030, USA

Cancer has proven to be an extremely difficult challenge to treat. Several fundamental issues currently underlie cancer treatment, including differentiating self from nonself, functional coupling of the recognition and therapeutic components of various therapies, and the propensity of cancerous cells to develop resistance to common treatment modalities via evolutionary pressure. Given these limitations, there is an increasing need to develop an all-encompassing therapeutic that can uniquely target malignant cells, decouple recognition from treatment, and overcome evolutionarily driven cancer resistance. We describe herein a new class of programmable self-assembling double-stranded RNA (dsRNA)-based cancer therapeutics that uniquely targets aberrant genetic sequences and in a functionally decoupled manner, undergoes oncogenic RNA-activated displacement (ORAD), initiating a therapeutic cascade that induces apoptosis and immune activation. As a proof of concept, we show that RNA strands targeting the EWS/Fli1 fusion gene in Ewing sarcoma cells that are end blocked with phosphorothioate bonds and additionally sealed with a 2′-deoxyuridine (2′-U)-modified DNA protector can be used to induce specific and potent killing of cells containing the target oncogenic sequence but not wild type.

INTRODUCTION

Cancer is the second-leading cause of death globally and was responsible for 8.8 million deaths in 2015, according to the World Health Organization.[1] Currently, the gold standard of care for cancer is some combination of chemotherapy, hormonal therapy, targeted molecular therapy, radiation, and/or surgical resection. However, each of these approaches is, to varying degrees, nonspecific, leading to undesirable side effects on healthy tissue.[2] In addition, with many of these therapies, especially targeted molecular therapy, the method of recognition and method of efficacy are intricately coupled. As a result, the choice of target affects the efficacy of therapy, often producing suboptimal results.[2] A good example of this is antisense small interfering RNA (siRNA) technology. siRNA is highly specific, targeting strands with sequence complementarity to the therapeutic silencing RNA strand; however, the mechanism of action of siRNA involves cleaving and degrading the target strand. It is entirely possible that the unique cancerous sequence being targeted is not essential for driving the cancerous phenotype, and so, its degradation has limited benefits. One of the last major issues with conventional therapies is that evolutionary pressure often drives cancerous cells to adopt a resistant phenotype leading to refraction/remission.[3] Given these limitations, there is an increasing need for a new class of all-encompassing cancer therapeutics that can uniquely target malignant cells, decouple recognition from treatment, and circumvent cancer resistance.

A fundamental difference between malignant cells and normal tissue is the presence of genetic mutations. Unique mutations can be identified during the pathological staging of biopsy samples using mutation panels or next-generation sequencing.[4,5] A method of targeting these genetic mutations, possibly multiple at once, represents an ideal form of personalized medicine and would allow for the selective identification of cancerous cells. Here, we describe a new class of RNA-based cancer therapeutics, called ORAD (oncogenic RNA-activated displacement), which targets mutated cancerous mRNA in a selective and programmable manner based on simple Watson-Crick thermodynamic base-pairing rules.

The ORAD system is composed of a targeting RNA strand and a complementary DNA protector. As depicted in Figure 1, when the RNA/DNA duplex encounters a wild-type strand with insufficient complementarity, the DNA protector fails to release, leading to no response. However, when the targeted cancerous sequence is encountered, the cancerous mRNA is able to dislodge the DNA protector via strand displacement, producing a therapeutic double-stranded RNA (dsRNA) product. We found that by end blocking the targeting RNA with phosphorothioate (PS) bonds to prevent nonspecific degradation and modifying the DNA protector with 2′-deoxyuridine (2′-U) residues to render the RNA/DNA duplex inert prior to opening, premature activation of the ORAD system in cells not harboring the target oncogenic sequence can be prevented.

Received 1 February 2020; accepted 28 July 2020;
https://doi.org/10.1016/j.omto.2020.07.013.

Correspondence: Vishwaratn Asthana, Department of Bioengineering, Rice University, Houston, TX 77030, USA.
E-mail: asthana.vishwaratn@gmail.com

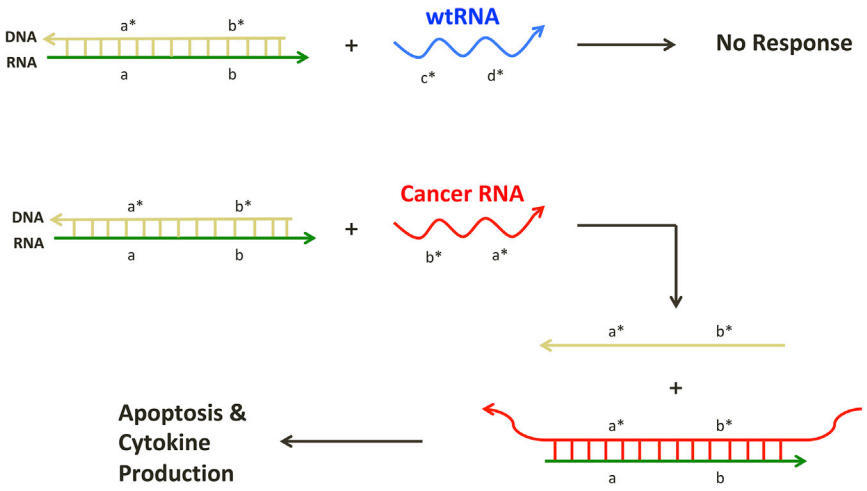

Figure 1. Oncogenic RNA-Activated Displacement (ORAD) Schematic

The ORAD system is composed of a targeting RNA strand and a complementary DNA protector. When the RNA/DNA duplex encounters a wild-type strand with insufficient complementarity, the DNA protector fails to release, leading to no response. However, when the targeted cancerous sequence is encountered, the cancerous mRNA is able to dislodge the DNA protector via strand displacement, producing a therapeutic dsRNA product leading to apoptosis and cytokine production. Arrowheads signify 3′ ends. Asterisks signify complementarity.

In general, RNA/RNA base pairing is more thermodynamically favorable than RNA/DNA base pairing, enabling DNA protector displacement in the presence of a cancerous mRNA target, even though their sequences are almost entirely homologous.[6–10] The use of a DNA protector to confer selectivity was first demonstrated by Zhang et al.[11] and has been validated to ensure near-optimal specificity across the diverse concentrations, sequence compositions, and salinities that may be encountered intracellularly. An in-depth explanation of the probe-protector system can be found in the Supplemental Information.

Long dsRNA or more precisely, strands greater than 30 base pairs (bp) are considered foreign elements in eukaryotic cells.[12] dsRNA is typically found among viruses possessing dsRNA genomes or dsRNA intermediates during replication. Accordingly, higher-level organisms have adopted mechanisms of identifying long dsRNA and responding to the infectious source.[13] In humans, several key proteins recognize long dsRNA. These include protein kinase R (PKR), Toll-like receptor 3 (TLR3), melanoma differentiation-associated protein 5 (MDA5), retinoic acid-inducible gene I (RIG-I), and 2′-5′-oligoadenylate synthase (OAS). PKR is an intracellular protein that binds dsRNA in a length-dependent fashion and induces apoptosis in the host cell to prevent viral propagation.[12] TLR3, MDA5, and RIG-I also recognize dsRNA and play an active role in immune activation. TLR3 is a surface receptor expressed primarily on antigen-presenting cells, whereas MDA5 and RIG-I are cytoplasmic helicase receptors expressed in almost all cell types. These three proteins function in innate immunity by recognizing dsRNA and activating nuclear factor (NF)-κB or interferon (IFN) regulatory factors, leading to production of inflammatory cytokines, such as type I IFNs.[14–21] RIG-I and MDA5 also possess caspase recruitment domains (CARDs), capable of inducing apoptosis when activated.[22] Lastly, OAS, in response to dsRNA, produces 2′-5′-oligoadenylates, which activate ribonuclease L (RNase L), leading to the destruction of both viral and endogenous mRNA in the cell.[23,24]

By producing a long dsRNA product, the ORAD system falsely alerts the cell, and possibly whole body, of a potential viral infection via the aforementioned dsRNA-sensing pathways. Activation leads not only to apoptosis of the target cancer cell but also to stimulation of the immune system (via activation of NF-κB or IFN regulatory factors) and subsequent production of inflammatory cytokines. Apoptosis and immune activation represent two independent therapeutic pathways induced by distinct, yet slightly overlapping, dsRNA-sensing pathways, providing a potential means to subvert evolutionarily driven cancer resistance. In addition, by producing a long dsRNA in the presence of a unique cancer marker, the ORAD scheme functionally decouples recognition from therapy by eliciting a therapeutic effect that is independent of the cancer marker being targeted. This permits the targeting of virtually any uniquely transcribed cancer mRNA with a known sequence.

As a starting cancer model, we have chosen Ewing sarcoma, an extremely malignant tumor of the bone and soft tissue with an extensively studied fusion gene. Sequences with closer homology to their wild-type counterpart, such as small nucleotide polymorphisms (SNPs), are more difficult to distinguish using ORAD, due to the marginal thermodynamic difference between the intended target and wild type. Cancerous fusion genes and their functional transcripts, however, contain a very distinct nucleotide sequence around the fusion site, representing an ideal starting point to test ORAD, due to the large thermodynamic difference between the intended target and wild type. A total of 358 gene fusions have been identified, to date, spanning all of the main subtypes of human neoplasia. These gene fusions account for approximately 20% of human cancer morbidity.[25,26]

Regarding Ewing sarcoma, approximately 90% of cases contain a t(11;22)(q24;q12) chromosomal translocation, resulting in the fusion of the EWS RNA binding protein 1 (EWSR1 also known as EWS) gene on chromosome 22 with the Fli-1 proto-oncogene, ETS transcription factor (FLI1) gene on chromosome 11.[27] The EWS/FLI1 fusion gene produces a functional mRNA transcript that is ultimately translated into the EWS/FLI1 oncogenic fusion protein. Proof-of-concept tests on the A-673 human Ewing sarcoma cell line, which expresses the EWS/Fli1 fusion transcript, and corresponding WPMY-1 wild-type cells using ORAD, reveal the potency and selectivity of the system and its potential as an all-encompassing cancer therapeutic.[28]

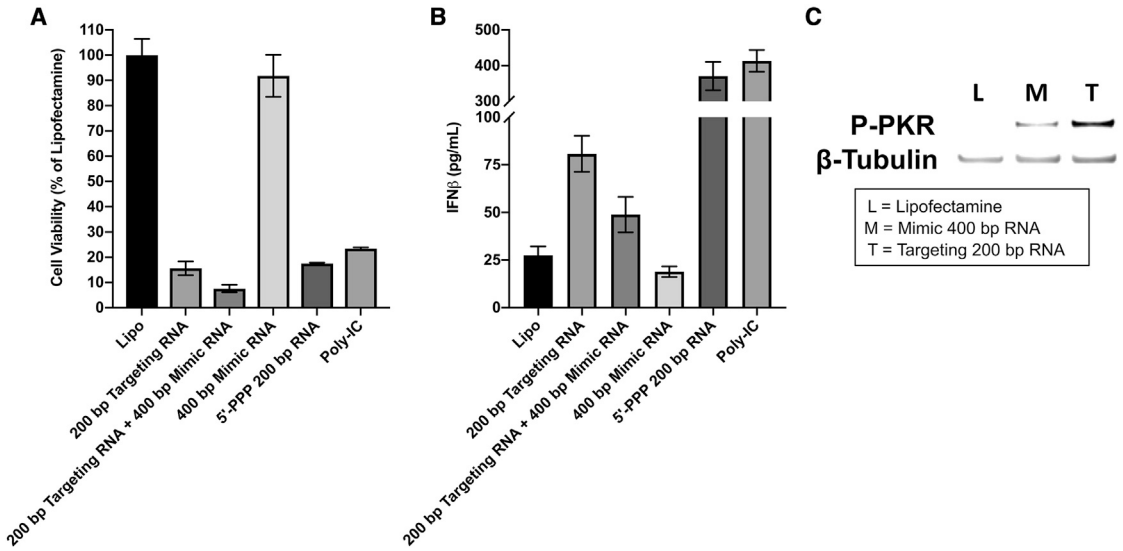

Figure 2. Assessing the Cytotoxic and Immunogenic Potential of the ORAD System

(A and B) Cytotoxicity (A) and IFN-β cytokine-induction (B) levels of 200 bp EWS/Fli1 targeting RNA were compared with levels generated by a reference 400-bp EWS/Fli1 sense RNA strand, as well as two established positive controls: poly(I:C) and 5′-triphosphate in A-673 cells. (C) Activation and subsequent phosphorylation of the dsRNA-sensing protein PKR (P-PKR) was measured in the presence of lipofectamine (L), 400 bp EWS/Fli1 mimic (i.e., sense) RNA (M), or 200 bp EWS/Fli1 targeting RNA (T), using western blot. Error bars represent the standard deviation of replicate conditions.

RESULTS

Determining the Cytotoxic and Immunogenic Potential of the ORAD System

It has been shown that dsRNA-binding proteins, like PKR, respond synergistically to multimonomer binding, with longer strands, likely producing a stronger response.[12] Preliminary tests suggest that *in vitro*-transcribed (Figure S1) EWS/Fli1 antisense targeting RNA strands, 200 bp in size, with 100 bp of the targeting RNA strand complementary to the EWS portion of the EWS/Fli1 fusion mRNA and the other 100 bp complementary to the Fli1 portion, were the most potent out of a range of targeting RNA varying in length from 20 bp to 390 bp (Figure S2). These 200 bp EWS/Fli1 targeting RNA were delivered without a DNA protector into A-673 cells, which express the target EWS/Flil1 mRNA, to assess the cytotoxic potential of the system (Figure 2A). They were also tested against a reference *in vitro*-transcribed, 400-bp RNA sense strand, which is a truncated mimic of the EWS/Fli1 mRNA transcript, as well as two established positive controls: 5′-triphosphate and poly-inosinic:polycytidylic acid (poly(I:C)). The 200-bp targeting RNA is shown to be extremely potent, inducing a greater than 80% reduction in cell viability, whereas the reference 400 bp RNA sense strand is nontoxic. At this targeting RNA length, we can expect PKR, RIG-I, and OAS to be active but not MDA5, which tends to activate in the presence of significantly longer dsRNA, typically kilobases or larger.[29–31]

IFN-β production was then assessed using supernatant from the treated wells (Figure 2B). IFN-β is a type I IFN that serves an important role in cancer immunotherapy and is a relatively sensitive marker of dsRNA pathway activation. In general, IFN-β induction levels closely mirror cytotoxic trends. To see if the ~10%–20% of cells that survived initial treatment were resistant to the ORAD system, we treated A-673 cells either once or twice with therapeutic RNA spaced by the appropriate incubation period (Figure S3). After 48 h, A-673 cell viability had been reduced by ~90%; however, a repeat administration and additional 48-h incubation reduce cell viability by another 95%, representing a greater than two order of magnitude drop in overall cell viability. These results not only indicate the extreme potency of the ORAD system but also imply that those cells that survive initial treatment have not developed resistance to the therapeutic RNA. To confirm dsRNA-specific pathway activation, PKR autophosphorylation was measured via western blot, revealing a robust and specific induction pattern in the presence of 200 bp EWS/Fli1 targeting RNA versus 400 bp EWS/Fli1 mimic (i.e., sense) RNA (Figure 2C). Altogether, data measuring cell viability, IFN-β expression, and PKR activation suggest that the generation of a long dsRNA product is indeed producing the robust response being observed.

Having validated the cytotoxic potential of the ORAD system, we ran strand-displacement simulations of the 200-bp EWS/Fli1 targeting RNA, now sealed with a DNA protector. Secondary structure analysis revealed that initial variants of the 200-bp targeting RNA/DNA, with the fusion site located directly in the middle of the strand (100 bp complementary to EWS and Fli1 each), were forming trimeric states with homologous wild-type sequences (Figure S4). To prevent this, the targeting fusion site was shifted toward the 3′ end of the targeting RNA in order to lock the strands kinetically (Figure S5).

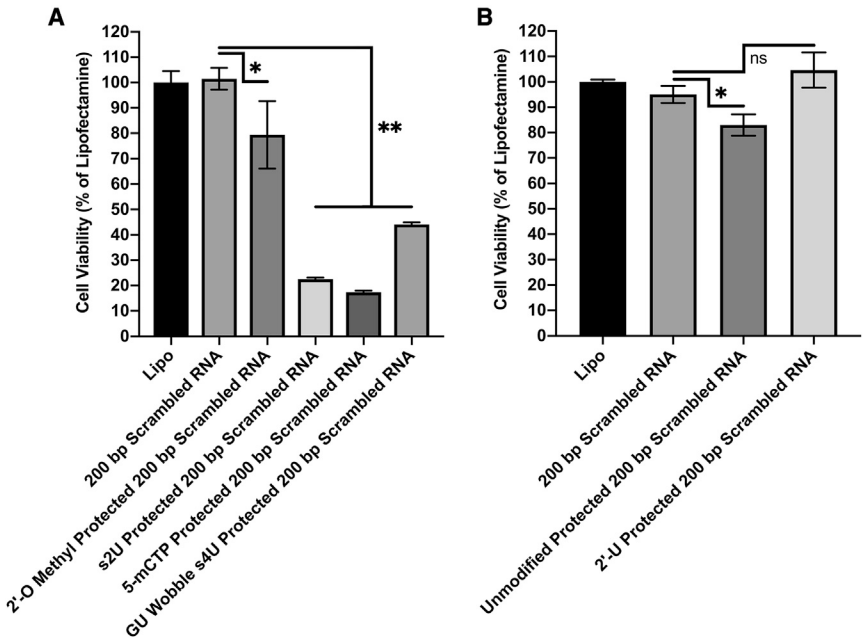

Figure 3. Chemically Modifying Protector Complexes to Prevent Nonspecific Cytotoxicity

(A and B) Scrambled 200 bp targeting RNA strands were protected with either modified (A) RNA or (B) DNA protectors and transfected into A-673 cells using lipofectamine. Only scrambled targeting RNA protected with 2′-U-modified DNA was rendered inert and nontoxic. s2U, 2-thiouridine; 5-mCTP, 5-methylcytidine; s4U, 4-thiouridine; 2′-U, 2′-deoxyuridine. Error bars represent the standard deviation of replicate conditions (*$p < 0.05$; **$p < 0.005$; ns, nonsignificant).

Modifying the Protector Seal to Prevent Nonspecific Cytotoxicity

Initial tests of the newly designed and synthesized EWS/Fli1 fusion-shifted targeting RNA strands in a wild-type WPMY-1 cell line, which does not express the EWS/Fli1 target mRNA, demonstrated nonspecific cytotoxicity when a DNA protector was utilized at a 1:1.5 targeting RNA-to-DNA protector ratio (data not shown). We hypothesized that the RNA/DNA hybrids of the ORAD system might function as a pathogen-associated molecular pattern (PAMP) and as a result, induce nonspecific immune activation. Accordingly, various modifications were tested on the protected RNA duplexes with the goal of rendering them fully inert. Whereas the modification of the targeting RNA could interfere with the therapeutic pathway of the ORAD system by altering binding to dsRNA-sensing proteins, the adaptation of the protector seal would be far less restrictive. Thus, several modified deoxynucleotides, ribonucleotides, and altered Watson-Crick base pairs that could potentially replace canonical bases and base pairs in the protector were compared to determine which modifications could help the duplex evade detection by PAMP receptors. These modified bases and altered base pairs include 2-thiouridine (s2U), 4-thiouridine (s4U), guanine-uracil (GU) wobble, 5-methylcytidine (5-mCTP), 2′-U, and 2′-O methyl.[32–34]

To avoid potential confounding effects from the EWS/Fli1 targeting RNA, we synthesized a new, 200-bp scrambled RNA strand, as well as corresponding modified RNA or DNA protectors, to isolate the protective effects of each modification. s2U-, 5-mCTP-, and GU wobble s4U-containing scrambled RNA protectors were synthesized using conventional RNA transcription, whereas 2′-U-containing scrambled DNA protectors were synthesized using a modified Taq PCR protocol. 2′-O methyl-containing DNA protectors cannot be enzymatically synthesized using PCR so strands modified with ~10% 2′-O methyl-containing guanosine triphosphates (GTPs) were chemically synthesized instead.

The newly synthesized scrambled duplexed strands were subsequently transfected into A-673 cells. We found that 2′-O methyl, s2U, 5-mCTP, or GU wobble with the s4U modification was not sufficient to shut down nonspecific cytotoxicity (Figure 3A). However, 2′-U-modified DNA proved to be almost completely inert (Figure 3B), making it the ideal protector modification moving forward for the RNA/DNA scheme.

EWS/Fli1 targeting RNA, now protected with 2′-U-modified DNA, was again tested in WPMY-1 control cells; however, preliminary results indicated that the DNA seal failed to confer any protective benefit (data not shown).

Modifying Targeting RNA to Resist Degradation

Two possibilities were considered regarding the failure of the new 2′-U-protected targeting RNA: either the targeting RNA was degrading in the cell cytoplasm, which would break the protector's kinetic lock, leading to premature activation of the ORAD system, or the inclusion of the 2′-U moiety altered base-pairing thermodynamics in a way that ultimately reduced the strength of the protector seal.

We first focused on inhibiting RNA degradation in the cytoplasm, via endo- and exonucleases, whereas minimizing alterations to the targeting RNA that could potentially reduce therapeutic efficacy.[35,36] Two candidate modifications were found that could potentially be used to inhibit RNA degradation: 2′-fluorination and PS-backbone incorporation.[37,38] Because endonucleases canonically cut at purine base residues, 2′-fluorine modifications at these sites should inhibit not only exonucleases but also endonucleases, even in the absence of a protector.[38] We hypothesized that end blocking RNA with PS bonds would inhibit exonucleases, whereas adding a DNA protector would protect against endonucleases, in the latter case, by forming a double-stranded nucleic acid complex.[37] The addition of DNA bases to the end of the targeting RNA strand should accentuate any protective benefit the PS bonds may confer. 2′-fluorinated RNA was synthesized

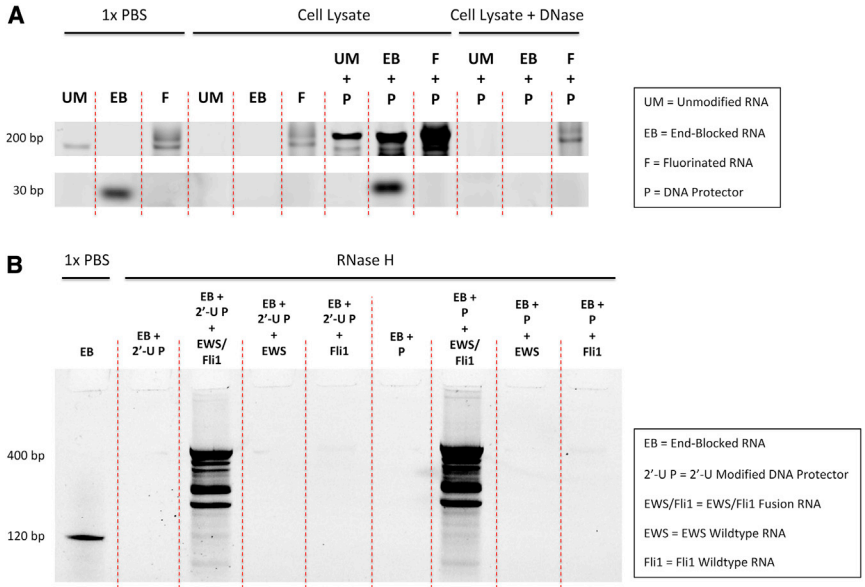

Figure 4. Modifying Targeting RNA to Resist Endo/Exonucleolytic Degradation and Assessing Selective Displacement Extracellularly

(A) 200 bp unmodified (UM), 30 bp chemically synthesized test-size end-blocked (EB), and 200 bp 2′-fluorinated (F) EWS/Fli1 targeting RNA were incubated alone or protected with DNA (P) in either 1 × PBS or WPMY-1 cell lysate for 48 h. Postincubation, select samples were digested with DNase to remove the overlapping signal from the DNA protector. All conditions were then run on a denaturing PAGE-urea gel and visualized using SYBR Gold. The presence of a DNA protector prevents degradation of end-blocked targeting RNA but not unmodified targeting RNA, whereas 2′-fluorination protects targeting RNA even in the absence of a DNA protector. It should be noted that the chemically synthesized end-blocked RNA, already shortened due to synthetic length restraints, is no longer visible post-DNase digestion, because the ends of the end-blocked RNA contain DNA, which when degraded in the presence of DNase, causes the RNA band to shift downward and off the gel. (B) After the establishment of end-blocked targeting RNA as a viable candidate, 120 bp 2′-U (2′-U P) and unmodified (P), DNA-protected end-blocked and fluorescently labeled EWS/Fli1 targeting RNA were incubated with 400 bp copies of EWS/Fli1, EWS, and Fli1 mRNA for 48 h in 1 × PBS. The displaced strands were then treated with RNase H and subsequently run on a denaturing PAGE-urea gel. RNase H should only degrade targeting RNA that is not displaced by the 400 bp RNA transcripts.

using the Y639F mutant T7 RNA polymerase, which is able to incorporate noncanonical bases, like 2′-fluoro (2′-F).[39] PS bonds cannot be incorporated using conventional transcription, so end-blocked PS strands were chemically synthesized.

To test the resistance of the modified strands to degradation, 200 bp unmodified RNA; 200 bp fluorinated RNA; or chemically synthesized, shortened (30 bp test-size) end-blocked RNA were incubated in the WPMY-1 cell lysate for 48 h. After incubation, strands were run on a denaturing PAGE-urea gel and stained with SYBR Gold (Figure 4A). The RNA strands alone are stable in 1× phosphate-buffered saline (PBS) over 48 h but almost entirely break down in the presence of cell lysate, with the exception of fluorinated RNA. As expected, in its protected state, the end-blocked RNA is also resistant to degradation. DNase was used to remove the overlapping signal from the DNA protector, revealing the fluorinated RNA underneath and further showing that DNA protection alone is insufficient to protect unmodified RNA in cell lysate. It should be noted that the chemically synthesized, 30-bp test-size end-blocked RNA is no longer visible post-DNase digestion, because the ends of the end-blocked RNA contain DNA, which when degraded in the presence of DNase, causes the RNA band to shift downward and off the gel.

After running preliminary cytotoxicity tests in cells, the 2′-F RNA that we synthesized was found to be too nonspecifically toxic (data not shown) and was not pursued further, leaving the end-blocked RNA as the primary candidate moving forward. By design, the end-blocked RNA contains two to three PS bonds at either end, along with four to five overlapping DNA bases. Because PS-modified RNA strands need to be chemically synthesized using phosphoramidite solid-phase synthetic processes, they can be made no longer than 120 bp with current technology.[40]

Having addressed the degradation issue, we next sought to verify that the 2′-U-protected end-blocked targeting RNA still followed thermodynamic simulations and bound only to the target EWS/Fli1 mRNA cancerous sequence and not the EWS or Fli1 mRNA wild-type sequences. This was accomplished using an RNase H assay to gauge selective displacement (see Figure S6 for a schematic). RNase H is an endonuclease that cleaves the RNA strand in an RNA/DNA duplex. Because the DNA protector seal is supposed to remain bound to the targeting RNA in the presence of both wild-type sequences, the RNA/DNA duplex remains a substrate for RNase H, leading to targeting RNA degradation. However, in the presence of the target cancerous sequence, the DNA protector is displaced, leading to the formation of a dsRNA complex, which is not an adequate substrate for RNase H. Accordingly, the targeting RNA remains intact and available for subsequent detection.

The protected end-blocked RNA were incubated in the presence of either the desired EWS/Fli1 target sequence or the EWS or Fli1 wild-type sequences for 48 h in 1× PBS and then treated with RNase H (Figure 4B). Only EWS/Fli1 RNA is capable of displacing the DNA seal, indicated by resistance to RNase H digestion and corresponding preservation of the fluorescent signal. EWS and Fli1 wild type are incapable of removing the DNA protector, leading to RNase H digestion and loss of signal. No difference in protector performance can be seen between the 2′-U and unmodified DNA protectors, signifying that 2′-U-modified bases do not have significantly altered base-pairing thermodynamics. Altogether, this suggests that RNA degradation

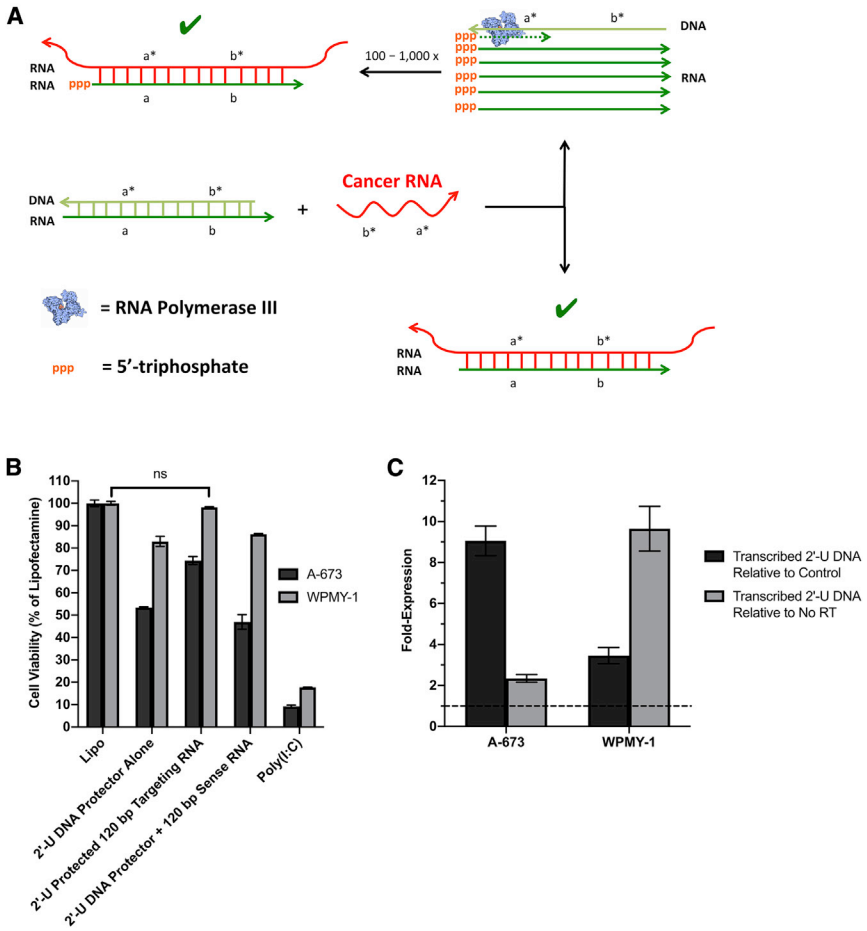

Figure 5. Conferring Specificity Using 2′-U DNA-Protected EWS/Fli1 Targeting RNA

(A) Hypothesized mechanism of targeting RNA and 2′-U DNA protector-induced cytotoxicity. In target cancer cells, cancerous mRNA is able to break the protector seal of the ORAD system and bind to the targeting RNA producing a dsRNA product that activates all of the established dsRNA pathways. By binding to the targeting RNA, however, the 2′-U DNA protector is released, making it a potential substrate for RNA polymerase III. The 2′-U DNA protector then serves as a template for the transcription of hundreds to thousands of potential RNA transcripts that are similar in sequence to the targeting RNA, ultimately amplifying the cytotoxic potential of the ORAD system. The presence of 5′-triphosphate on the transcribed RNA only serves to enhance the effect. (B) 2′-U DNA-protected, 120-bp end-blocked EWS/Fli1 targeting RNA strands, complexed at a 1:1 ratio by mass, were transfected into A-673 and WPMY-1 cells using lipofectamine. When complexed at a 1:1 ratio, cell viability in WPMY-1 approaches nontoxic levels with cytotoxicity still apparent in A-673 cells. The use of a noncomplementary EWS/Fli1 sense RNA strand with the sense 2′-U DNA protector confers no protective benefit in WPMY-1 cells (ns, nonsignificant). (C) qRT-PCR was used to quantify transcribed RNA expression levels of the EWS/Fli1 2′-U DNA protector in treated cells. In both A-673 and WPMY-1 cells, a weak but significant (greater than unity which is indicated by the dotted line) transcribed 2′-U DNA signal is apparent that exceeds both the nonspecific signal from control, untreated cells, as well as a signal that originates from DNA, the latter of which was determined by running a no-reverse-transcriptase (RT) control. Error bars represent the standard deviation of replicate conditions. Arrowheads signify 3′ ends. Asterisks signify complementarity.

in the cell cytoplasm and breaking of the protector's kinetic lock likely led to premature activation of the 2′-U DNA-protected targeting RNA strands in the control WPMY-1 cells and that this process can be inhibited by end blocking the targeting RNA.

Testing and Characterizing 2′-U-Protected End-Blocked Targeting RNA

Observational data of early tests utilizing the 2′-U EWS/Fli1 DNA protector were surprising in that the EWS/Fli1 2′-U DNA protector alone was found to induce cytotoxicity, which was not the case with the scrambled 2′-U DNA protector tested earlier. We realized that if 2′-U DNA-mediated cytotoxicity was sequence specific, it is theoretically possible that the sense 2′-U DNA protector is getting transcribed in the cytoplasm into antisense targeting RNA, via an RNA polymerase. Recently, RNA polymerase III, which is typically thought to reside in the nucleus, was found localized in the cytoplasm functioning as a DNA sensor.[41] When displaced from the RNA/DNA duplex by the target cancer mRNA sequence, the 2′-U DNA protector is potentially made available for transcription by RNA polymerase III, leading to linear amplification of the targeting RNA strand and increased potency of the ORAD system (Figure 5A).

With the 2′-U DNA protector potentially more cytotoxic than the targeting RNA strand but partially uncomplexed as part of the initial RNA/DNA duplex ratio of 1:1.5, an adjustment was made lowering the duplex ratio down to 1:1. Through these changes, the DNA protector of the ORAD system demonstrated intracellular specificity for the first time (Figure 5B). As expected, the 2′-U DNA protector alone was toxic in the A-673 and WPMY-1 cells, but when duplexed at a 1:1 ratio with targeting RNA, cell viability in WPMY-1 returned to near 100%, with cytotoxicity still apparent in the A-673 cells. Perhaps most convincing is the complexing of the 2′-U DNA protector with a noncomplementary sense RNA strand. The sense RNA strand cannot seal the 2′-U DNA protector, causing the cytotoxicity profile for this condition to closely mirror the 2′-U DNA protector-alone condition. Supernatant from the treated wells was also extracted and tested for IFN-β production. When the targeting strands are protected, IFN-β is potently induced in the A-673 target cell line versus the control WPMY-1 cells (Figure S7). It should be noted that the cytotoxic potential of the ORAD system appears to have been reduced after shortening the size of the targeting RNA to 120 bp from 200 bp, as well as end blocking the RNA with both DNA bases and PS bonds.

The previously reported data strongly support the RNA polymerase III hypothesis, although not directly. In an attempt to prove mechanistically RNA polymerase III activity, we sought to detect and quantify the transcribed RNA product that the 2′-U DNA protector would generate in the presence of RNA polymerase III using qRT-PCR. In both A-673 and WPMY-1 cells, a weak but significant (greater than unity) transcribed 2′-U DNA signal was detected that exceeds both a nonspecific signal from control, untreated cells, as well as a signal that originates from DNA, the latter of which was determined by running a no-reverse transcriptase control (Figure 5C). In target A-673 cells, this signal was approximately 9-fold higher than the corresponding control condition, and in WPMY-1, this signal was approximately 3.5-fold higher.

DISCUSSION

The proof-of-concept ORAD system described herein represents a potentially new class of cancer therapeutics based on the principle of self-assembling dsRNA. The system is a potent inducer of both cytotoxicity and cytokine production and can selectively target cancerous cells that express unique fusion genes, while sparing normal tissue. By producing a long dsRNA product in the presence of a unique cancer marker, the ORAD scheme functionally decouples recognition from therapy by eliciting a therapeutic effect that is independent of the cancer marker being targeted. This permits the targeting of virtually any uniquely transcribed cancer mRNA with a known sequence.

A similar approach has been attempted before using 40 bp antisense RNA strands designed to be complementary to fragments flanking the fusion site of an oncogene.[42] When bound to the target oncogene but not wild-type mRNA, a dsRNA product sufficient in length to activate PKR is generated. One of the issues with this approach, however, is that the length of antisense RNA used must be restricted, which would likely reduce potency. Furthermore, the antisense RNA needs to be constitutively expressed at high levels using a transfected plasmid.[42] Another method using RNA hairpin displacement has been attempted but met with limited success.[43] RNA hairpins are generally less stable and consistent than the protected probe scheme listed here, often leading to increased nonspecific activation and off-target effects.[11] Lastly, use of preformed dsRNA or poly(I:C), especially as an immune adjuvant in clinical trials, has become increasingly popular. However, targeting and specificity require the expression of unique extracellular antigens that homing vectors can target.[44,45] It is possible that these unique antigens are not be available for targeting, are also expressed on healthy cells, or are downregulated as a form of evolutionary resistance, limiting the potential use of this form of therapy. By virtue of its design, the ORAD system overcomes many of the aforementioned issues.

We show that *in vitro*-transcribed targeting RNA strands, 200 bp in length, can reduce cell viability by up to 90% in cells that express a target cancer fusion mRNA sequence, whereas an equivalent dose of unprotected, 400 bp EWS/Fli1 mimic (sense) RNA, intended to serve as a negative control, is minimally toxic. This suggests that the potent response induced by the 200-bp EWS/Fli1 is, in part, governed by sequence specificity and not the result of off-target binding. In addition, the 200-bp ORAD targeting RNA was more cytotoxic than both 5′-triphosphate RNA and poly(I:C), which are strong inducers of RIG-I and PKR.[14,46] Supernatant extracted from treated wells shows that IFN-β induction levels closely mirror cytotoxic trends, with the exception of precomplexed, 200 bp EWS/Fli1 targeting RNA + 400 bp mimic RNA, which produced lower levels of IFN-β than expected. This is likely the result of the overwhelming cytotoxicity of the precomplexed dsRNA hindering the production of IFN-β. Selective PKR activation in the presence of 200 bp targeting RNA was observed via detection of phosphorylated PKR protein, whereas 400 bp mimic RNA showed only slight, nonspecific activation, most likely via the formation of minimal, noncontiguous intramolecular dsRNA segments generated via secondary hairpin formation. Unfortunately, a robust method to detect other endogenously activated dsRNA-sensing proteins, including RIG-I and OAS3, could not be established in the current experimental framework. Altogether, the data indicate that the formation of a dsRNA product is indeed responsible for producing the pronounced response that is being observed.

Literature suggests that in the 100- to 200-bp-size range, we can expect several dsRNA-sensing pathways, including PKR, RIG-I, OAS, and Dicer, to activate but not MDA5.[47] It is possible that targeted cytotoxicity may be even more pronounced at significantly longer targeting RNA lengths by recruiting additional dsRNA-sensing proteins. By activating multiple, somewhat redundant, dsRNA-sensing pathways that induce two distinct therapeutic pathways (apoptosis and immune activation), the ORAD system is potentially resilient to evolutionary resistance acquired either upstream or downstream of the recognition portion of the dsRNA signaling transduction cascade. Because cancerous mutations, especially driver mutations, are signatures of the cancerous phenotype and not easily downregulated, the ORAD system's recognition of unique cancer mRNA represents another means to prevent evolutionarily driven cancer resistance.[48] The ability to target multiple mutations at once only serves to strengthen this effect. This phenomenon is confirmed to an extent with the repeat transfection test that was conducted on cancer target cells that survived initial treatment. The initial 10% of cells that "evaded" ORAD-induced cytotoxicity were further reduced in number by approximately an order of magnitude upon repeat administration, likely indicating that those cells that survive initial treatment have not developed resistance to the therapeutic RNA. With multiple dosing regimens, cytotoxicity could theoretically reach 100%.

After demonstrating the success of long dsRNA in inducing cytotoxicity and activating the innate immune system, thus confirming the *therapeutic* arm of the ORAD system, we focused on engineering DNA protectors that would confer specificity to the targeting RNA strands in order to validate the *diagnostic* arm of the ORAD system. To maintain selectivity and prevent trimer formation, the ORAD RNA/DNA hybrids were modified so that the targeting RNA fusion

site was shifted toward the 3′ end of the strand, kinetically locking the system.

After running cytotoxicity studies of the newly designed and synthesized EWS/Fli1 fusion-shifted targeting RNA strands in control WPMY-1 cells, the DNA-protected targeting RNA complexes were found to be nonspecifically cytotoxic. We realized that the RNA/DNA hybrids of the ORAD system might function as a PAMP. In response to the very long cytoplasmic RNA/DNA duplexes that were exogenously being introduced into the cell, inflammasomes, including the NLRP3 inflammasome, might be triggering and inducing nonspecific cytotoxicity. The NLRP3 inflammasome has been shown to recognize RNA/DNA hybrids of bacterial origin that have gained access to the cytoplasm. Upon recognition and activation, NLRP3 inflammasomes induce the production of IL-1β, maturation of IL-18, and stimulation of a form of inflammatory cell death known as pyroptosis.[49,50] To render the RNA/DNA duplexes inert, various modifications to the protector were tested, including the incorporation of s2U, s4U, GU wobble, 5-mCTP, 2′-U, and 2′-O methyl. Only insertion of 2′-U modifications into the DNA protector rendered scrambled RNA/DNA duplexes nontoxic in A-673 cells. 2′-U is unique in that it contains structural components from both RNA and DNA. Whereas 2′-U has a DNA sugar lacking a 2′-hydroxyl, it contains an RNA uracil base. Although induction and subsequent resolution of PAMP activation were not directly assessed, 2′-U may create a hybrid structure that is not an adequate substrate for pathogen-detection systems in the cell, including not only the NLRP3 inflammasome but also traditional dsRNA-sensing pathways. Future studies investigating the specific components of the PAMP activation pathway, such as the NLRP3 inflammasome, will help elucidate their various contributions to cell viability and immunogenicity in the setting of the ORAD system. Ultimately, the ability of 2′-U to render the ORAD complexes inert makes it the ideal candidate moving forward for the RNA/DNA scheme.[51]

After testing fusion-shifted EWS/Fli1 targeting RNA, protected with newly synthesized 2′-U-modified DNA in WPMY-1 cells, we found that the DNA seal failed to confer any protective benefit. We speculated that either the targeting RNA was degrading in the cell cytoplasm, which would break the protector's kinetic lock, or that inclusion of the 2′-U moiety was reducing the strength of the DNA protector seal. We focused first on inhibiting RNA degradation, using either 2′-fluorination or PS-backbone incorporation. After synthesizing the appropriate strands, unmodified, fluorinated, and end-blocked PS-modified RNA were incubated in cell lysate for 48 h and run on a denaturing PAGE-urea gel. Unmodified RNA was susceptible to degradation regardless of whether it was duplexed with a DNA protector, whereas 2′-F was resilient to degradation with or without a protector seal. The end-blocked PS-modified RNA was only resistant to degradation when duplexed to the DNA protector, confirming the dominant role of exonucleases in degrading and potentially prematurely activating strands of the ORAD system.

Because 2′-F RNA was found to be too nonspecifically toxic, we were left with end-blocked PS-modified RNA as the primary candidate for protecting the targeting RNA of the ORAD system. By design, the end-blocked RNA contains two to three PS bonds at either end, along with four to five overlapping DNA bases. PS bonds substitute a sulfur atom for a nonbridging oxygen in the phosphate backbone of an oligonucleotide strand. This renders the internucleotide linkage resistant to nuclease degradation. However, the number of PS bonds that can be incorporated into a strand is limited due to nonspecific toxicity of the bonds.[37] An additional limitation is that these strands need to be chemically synthesized, limiting the size of the targeting RNA to no more than 120 bp.

Selective displacement of the newly synthesized 2′-U DNA-protected, 120-bp fusion-shifted end-blocked targeting RNA was then tested using an RNase H assay. The incubation of the strands in 1× PBS for 48 h with truncated *in vitro*-transcribed copies of the target EWS/Fli1 and wild-type EWS and Fli1 sequences confirms the specificity of the ORAD strands for the intended target, indicated by resistance to RNase H digestion and corresponding preservation of the fluorescent signal with the EWS/Fli1 target sequence and loss of signal due to RNase H digestion in the presence of the EWS and Fli1 wild-type sequences. The complex band pattern observed between 120 bp and 400 bp in the presence of EWS/Fli1 is likely due to abnormal migration of the thermodynamically stable but partially dsRNA complex (120 bp is duplexed fully, whereas 280 bp is single stranded). An extended discussion regarding the RNase H displacement assay can be found in the Supplemental Information.

Having modified the ORAD strands to prevent premature activation in the cell cytoplasm, we tested various combinations of the newly modified end-blocked 120-bp synthetic EWS/Fli1 targeting RNA with a complementary 2′-U DNA protector to assess any effects that alterations to the RNA would have on cytotoxicity. Interestingly, we noticed that the EWS/Fli1 2′-U DNA protector alone was inducing cytotoxicity, which was not the case with the scrambled 2′-U DNA protector used in Figure 3. We hypothesized that an additional enzyme—RNA polymerase III—may be contributing to the toxicity of the 2′-U DNA by transcribing it in the cytoplasm into what is effectively targeting RNA. RNA polymerase III is typically thought to reside in the nucleus where it transcribes rRNA, tRNA, and other small RNAs.[52] However, recent literature suggests that RNA polymerase III is also localized in the cytoplasm where it functions as a DNA sensor, transcribing foreign DNA into RNA with a 5′-triphosphate, which can subsequently be detected by RIG-I. In particular, sequences rich in adenine- and thymine-base residues were found to be adequate substrates for RNA polymerase III in the cytoplasm.[41] Although it is not clear how, 2′-U may function similarly.

Based on the proposed interaction between RNA polymerase III and the ORAD system, depicted in Figure 5A, both the 2′-U DNA and targeting RNA can be viewed as primary therapeutic components, with each serving as the protector for the other. Accordingly, the targeting RNA-to-DNA protector ratio was brought down from 1:1.5 (DNA

protector in 0.5× excess) to 1:1 (DNA protector present in equimolar amounts). For the original ratio, which had the 2′-U DNA protector in 50% excess of the targeting RNA, a small but nontrivial percent of 2′-U DNA was left uncomplexed, making it available for potential transcription.

With the 1:1 RNA-to-DNA ratio adjustment, we observed the resolution of nonspecific cytotoxicity in WPMY-1 cells, suggesting that the RNA and DNA strands of the ORAD system were now appropriately sealed and inert in control cells. The sequence-specific effect of the protector complex was confirmed using a noncomplementary sense RNA strand in conjunction with the 2′-U DNA protector, which together, was inadequate to seal the duplex and prevent cytotoxicity. It should be noted that the cytotoxicity of the 2′-U-protected targeting RNA is slightly reduced in A-673 cells relative to the 2′-U DNA protector alone when it should theoretically remain unchanged. We suspect that the displacement reaction is not 100% complete in the target cell line and that further tuning of the toehold regions may be required. In addition, the reduced length of the targeting RNA, as well end blocking with both PS bonds and DNA bases, appears to have notably reduced overall cytotoxicity. Whereas reducing the length of the targeting RNA can theoretically reduce the cytotoxic potential of the ORAD system by decreasing the number of dsRNA-binding monomers that can attach to the final targeting RNA complex, it is not clear why end blocking the strands is also inhibitory. It is possible that certain dsRNA-sensing proteins are incapable of accessing the ORAD targeting RNA when end blocked. Although crystal structures of PKR suggest that the protein is capable of binding dsRNA internally, helicases, like RIG-I, may need to initiate binding at the 5′ or 3′ ends of the strand.[53–56] Although end-modification incorporation is currently necessary to prevent RNA degradation, and chemical synthesis is required to insert these modifications, thereby limiting the size of the targeting RNA, it may be possible in the near future to synthesize chemically longer strands, incorporate end-blocking modifications via *in vitro* transcription, or utilize a different set of end-blocking modifications that minimally alter the targeting RNA strand to preserve cytotoxicity at levels seen in Figure 2A, whereas simultaneously maintaining specificity.

In an attempt to prove mechanistically the RNA polymerase III mechanism, qRT-PCR was used to detect and quantify the transcribed RNA product that the 2′-U DNA protector would generate in the presence of RNA polymerase III. After running total RNA extraction on A-673 and WPMY-1 cells treated with and without the EWS/Fli1 2′-U DNA protector, incubating the extract with uracil-DNA glycosylase (UDG) to remove 2′-U DNA, as well as DNase to remove genomic DNA, and running gene-specific primer qRT-PCR, we detected a trace (greater than unity) but unique RNA signal in cells treated with the 2′-U DNA protector versus untreated control cells. The transcribed RNA signal was also stronger than any signal originating from DNA, which was determined by running a no-reverse transcriptase control. To ensure that the signal enhancement seen in the 2′-U DNA protector condition versus untreated control was not the result of changes in Fli1 expression levels, a modified 2-step qRT-PCR was performed, confirming the identity of the amplified product as the RNA-transcribed 2′-U DNA (Figure S8).

The aforementioned data strongly support the RNA polymerase III hypothesis, albeit indirectly. If the proposed interaction of the ORAD system with RNA polymerase III is indeed true, it would raise the cytotoxic potential of the system considerably, due to the linear amplification of the therapeutic agent. In addition, even though RNA polymerase III potentially enhances the cytotoxicity of the system, it is not essential. For cancerous cells that do not express RNA polymerase III or have it knocked down as a form of evolutionary resistance, the primary targeting RNA strand is still present to enact the original design of the system. More studies are required to verify the RNA polymerase III hypothesis or determine possible alternative mechanisms by which 2′-U DNA is transcribed intracellularly. Additional work is also necessary to establish the precise role of chemical modifications and sequence of the DNA protector in the transcription potential of exogenous ORAD DNA in the cytoplasm. Further exploration of the proposed 2′-U mechanism may elucidate novel therapeutic targets or future avenues for cancer treatment.

Conclusions

ORAD represents a proof-of-concept system to induce specific and potent killing of cells containing a target oncogenic sequence but not wild-type, decouple recognition from treatment, and overcome evolutionarily driven cancer resistance. With further advances in RNA synthesis methodology, including but not limited to chemical synthesis of longer strands or ability to incorporate end-blocking modifications via *in vitro* transcription, ORAD treatment with longer 2′-U DNA-protected targeting RNA and an appropriate delivery vehicle has the potential to induce a robust response *in vivo* and one day improve progression-free and/or overall survival in the setting of a clinical trial. In addition, whereas gene fusions were the focus of this study, it is theoretically possible to extend ORAD targeting to SNPs.

In theory, the targeting strands of the ORAD system only need to be administered once, as immune surveillance and memory can suppress tumor recurrence and metastasis. However, if a tumor were to recur, this form of personalized medicine can be repeated as long as a biopsy and genomic sequence are attainable.[57] The ability to potentially target any cancer type is also strongly compelling. We hope our self-assembling dsRNA cancer therapeutics will one day improve the survival and quality of life for cancer patients and introduce a paradigm shift in how we view and treat cancer, by placing a special emphasis on what makes cancer fundamentally unique—genetics.

MATERIALS AND METHODS

RNA Synthesis

RNA was transcribed using the HiScribe T7 high-yield RNA synthesis kit (New England Biolabs), according to the manufacturer's instructions. To prevent the formation of aberrant dsRNA products during T7 RNA transcription, the concentration of $MgCl_2$ was limited to 6 mM.[58] 100 ng of DNA gBlock (Integrated DNA Technologies

[IDT]) containing the T7 promoter was used as template and transcribed for 48 h at 37°C. The post-transcription reaction mixture was incubated with 10 units of DNase I (New England Biolabs) at 37°C for 1 h to remove the gBlock template and then purified using an RNA spin column (Zymo Research). Purified RNA was then treated with 200 units of calf intestinal phosphatase (New England Biolabs) at 37°C for 24 h to ensure complete removal of any 5′-triphosphate moieties and then purified again using an RNA spin column (Zymo Research). Lastly, RNA yields were determined using a Qubit 3.0 fluorometer (Invitrogen).

For modified RNA synthesis, including s2U, s4U, GU wobble, and 5-mCTP, the natural base was replaced with its modified counterpart at equimolar concentrations and synthesized as described above. Targeting RNA strands end blocked with PS bonds were chemically synthesized by IDT. 2′-F-modified RNA was synthesized using the DuraScribe T7 transcription kit (Lucigen), as described in the manufacturer's protocol. A list of all sequences and primers used can be found in Table S1.

DNA Synthesis and RNA Protection Protocol

DNA was synthesized using standard Taq polymerase (New England Biolabs). For 2′-U scrambled DNA synthesis, a reverse primer-only approach was utilized: 5 μL 10× Taq buffer, 1 μL each of 10 mM deoxyribonucleotide triphosphate (dNTP; or 2′-U), 1 μL of 100 μM reverse primer only, 2 μL of 50 mM $MgCl_2$, 1 μL of 10 ng/μL DNA template, 1 μL of Taq DNA polymerase, and 36 μL of H_2O (50 μL total). The reaction mixture was then run through the following PCR protocol on the T100 thermal cycler (Bio-Rad): (1) denature at 95°C for 3 min, (2) denature at 95°C for 45 s, (3) anneal at 55°C for 30 s, (4) extend at 72°C for 1 min 30 s, (5) repeat steps 2–4 30 times, and (6) final extension at 72°C for 10 min. Samples were then purified using a DNA spin column (Zymo Research) and quantified using a NanoDrop apparatus (Thermo Fisher Scientific). DNA protector strands containing 2′-O methyl modifications were chemically synthesized by IDT.

For high-yield synthesis of 2′-U EWS/Fli1 DNA, the following modified Taq protocol was utilized with both forward and reverse primer: 5 μL 10× Taq buffer, 1 μL each of 10 mM dNTP (or 2′-U), 1 μL of 100 μM 5′-monophosphate-modified forward primer, 1 μL of 100 μM 5′ PS-modified reverse primer, 2 μL of 50 mM $MgCl_2$, 1 μL of 1 ng/μL DNA template, 1 μL of Taq DNA polymerase, and 35 μL of H_2O (50 μL total). The reaction mixture was then run through the same thermocycling protocol listed above. Synthesized product was subsequently purified using a DNA spin column and then digested using lambda exonuclease (New England Biolabs): 10 μL 10× lambda exonuclease buffer, 10 μL lambda exonuclease (50 units), 12 μL dsDNA template, and 68 μL H_2O (100 μL total) at 37°C overnight. Lambda exonuclease digestion is required to isolate the desired antisense DNA protector from a dsDNA PCR product. Because lambda exonuclease preferentially digests DNA with a 5′-monophosphate, the forward primer, designed to elongate the nondesired sense DNA strand, is modified with a 5′-monophosphate instead of 5′-hydroxyl. In addition, the reverse primer, designed to elongate the desired antisense DNA strand, is modified with six PS bonds on the 5′ end to inhibit exonuclease digestion.[37] Following lambda exonuclease treatment, strands were purified using a DNA spin column and then quantified using a NanoDrop apparatus.

To duplex and protect the targeting RNA strands, 0.15 μg/μL of DNA protector and 0.1 μg/μL of targeting RNA (1:1.5 ratio) were thermally annealed in 1× PBS using the T100 thermal cycler, based on the following protocol: samples were initially heated to 95°C for 5 min and then uniformly cooled to 20°C over the course of 1 h. For experiments testing and characterizing the 2′-U-protected end-blocked targeting RNA (Figure 5), 0.1 μg/μL of RNA was annealed with 0.1 μg/μL of DNA (1:1 ratio) to remove any excess, nonduplexed DNA protector.

Cell Viability and Cytokine Studies

A-673 and WPMY-1 cells were obtained from ATCC (American Type Culture Collection; Manassas, VA, USA) and maintained in Dulbecco's modified Eagle's medium (DMEM), supplemented with 10% fetal bovine serum (FBS) and 1% penicillin/streptomycin. Both cells were grown at 37°C in 5% CO_2. For plating, cells were trypsinized from their flasks and quantified manually using a bright-line hemocytometer (Sigma-Aldrich, St. Louis, MO, USA). Replicates of each dilution were then plated on either a 48- or 24-well Corning Costar flat-bottom cell-culture plate (Thermo Fisher Scientific, Waltham, MA, USA) at either 1×10^4 cells/well or 5×10^5 cells/well, respectively, and grown overnight. Cells were then transfected with nucleic acid (RNA and/or DNA) using Lipofectamine RNAiMax (Life Technologies) at a ratio of 0.3 μg nucleic acid/1 μL Lipofectamine. The total amount of nucleic acid added to each experimental well was 3.15 μg of RNA and/or DNA/50,000 cells, requiring approximately 10.5 μL of Lipofectamine RNAiMax to deliver this dose effectively. Experiments testing the chemically synthesized, 120-bp targeting RNA required double the nucleic acid/Lipofectamine dose to induce an appropriate response (a detailed discussion of ORAD dosing can be found in the Supplemental Information). After a 48-h incubation, cells were stained with 4′,6-diamidino-2-phenylindole (DAPI) and quantified using microscopic cytometry, as described previously.[59] For cytokine studies, supernatant was extracted from the cell plates just prior to cell staining and then processed and measured using a human IFN-β ELISA kit (PBL Assay Science).

For extended transfection studies, cells were plated onto 24-well cell-culture plates at 5×10^5 cells/well and then allowed to adhere overnight. Cells were transfected as described above and then given 48 h to incubate, after which, the media were replaced with fresh media with one PBS wash in between. Cells were transfected once again and given another 48 h to incubate, after which, cell viability was assessed.

Western Blot

A-673 cells were plated onto a 6-well cell-culture plate at 5×10^6 cells/well and then allowed to adhere overnight. Cells were transfected, as

described above, and then given 24 h to incubate. Following incubation, cells were lysed with radioimmunoprecipitation assay buffer (RIPA) buffer (Santa Cruz, CA, USA), as described in the manufacturer's instructions, and then centrifuged at 10,000 × *g* for 10 min to remove cell debris. Protein concentrations were calculated using a bicinchoninic acid (BCA) protein assay (Pierce), according to the manufacturer's instructions. Cell lysates (20 μg) were diluted in 4× lithium dodecyl sulfate (LDS) buffer (Life Technologies) with 5% beta-mercaptoethanol. Samples were denatured by heating to 95°C for 5 min and cooled to room temperature. Proteins were resolved by sodium dodecyl sulfate (SDS)-PAGE on 4%–12% gradient gels (Invitrogen) using 3-(*N*-morpholino)propanesulfonic acid (MOPS) running buffer (Life Technologies) and transferred to polyvinylidene fluoride (PVDF) membranes. Membranes were blocked for 1 h at 40 rpm on a shaking platform with a 2:1 ratio of Odyssey Blocking Solution (Li-Cor) to PBS with 0.05% Tween-20 (PBS-T).Phospho PKR (T446) antibody (Abcam; ab32036) and anti-β-tubulin (Developmental Studies Hybridoma Bank; E7) primary antibodies were diluted 1:1,000 in a solution of PBS-T with 0.1% bovine serum albumin (BSA). Primary antibodies were then detected using goat anti-rabbit 680 nm (Rockland Immunochemical; RL6111440020.5) and goat anti-mouse 800 nm secondary antibodies (Rockland Immunochemical; RL6111450020.5) respectively, after incubating in PBS-T + 0.1% BSA for 2 h. Membranes were imaged on an Odyssey Classic Imager (Li-Cor).

Cell Lysate Extraction

Cultured cells were brought into suspension using a standard cell-culture protocol, centrifuged at 250 × *g* for 5 min to form a cell pellet, and then washed once with PBS. Cells were subsequently resuspended in cell lysis buffer (920 μL H_2O, 50 μL 1 M Tris-HCl, pH 7.4, 10 μL 10% SDS, 10 μL Igepal CA-630, 8.77 mg NaCl, 5 mg sodium deoxycholate, and 10 μL protease inhibitor cocktail) at a ratio of 1 mL cell lysis buffer per 10^6 cells and then incubated for 15 min on an orbital shaker. Lysed cells were centrifuged at 12,000 × *g* for 10 min. The remaining supernatant is the cell lysate.

RNA Extraction and qRT-PCR

Cell lysate was extracted, after incubating cells for 24 h in condition, using the cell lysate extraction protocol listed above. Cell lysate was purified using a RNA spin column and then treated with UDG (5 μL UDG, 5 μL of 10× UDG reaction buffer, 25 μL purified cell lysate, and 15 μL of H_2O) (New England Biolabs) for 1 h at 37°C, followed by DNase I (10 μL DNase I, 10 μL of 10× DNase I buffer, 50 μL UDG-treated cell lysate, and 30 μL of H_2O) for 1 h at 37°C. Following UDG and DNase I incubation, samples were purified again using an RNA spin column.

After digestion of 2′-U and genomic DNA, RNA levels were quantified using either a conventional 1-step qRT-PCR or a modified 2-step qRT-PCR protocol, both using the iTaq Universal SYBR Green One-Step Kit (Bio-Rad). For 1-step qRT-PCR, the following reaction components were mixed together: 5 μL of 2× iTaq Universal SYBR Green Reaction Mix, 0.125 μL iScript reverse transcriptase, 0.5 μL of 10 μM forward and reverse primer, 1 μL cell lysate, and 2.875 μL H_2O. The qRT-PCR samples were then measured using the CFX96 Touch Real-Time PCR Detection System (Bio-Rad) using the following thermocycling protocol: (1) reverse transcribe at 50°C for 10 min, (2) denature DNA and activate Taq polymerase at 95°C for 1 min, (3) denature DNA at 95°C for 10 s, (4) anneal and extend at 62°C for 20 s, followed by fluorescence capture, and (5) repeat steps 3–4, 35 times.

Assessing RNA Stability in Cell Lysate and RNase H Displacement Assay

For assessing RNA stability in cell lysate, 2.5 μL of 0.1 μg/μL-protected or -unprotected targeting RNA was incubated in 2.5 μL of cell lysate at 37°C for 48 h. The digested samples were then mixed 1:1 (v/v) with formamide (Sigma-Aldrich) and run on a denaturing PAGE-urea gel (Thermo Fisher Scientific) in 1× Tris-borate-EDTA (TBE) buffer at 60°C.

For RNase H displacement assays, 1 μL of 0.05 μg/μL DNA-protected, fluorescently labeled targeting RNA was incubated with 1 μL of 0.1 μg/μL 400 bp EWS or Fli1 RNA in 1× PBS and incubated at 37°C for 48 h. Following incubation, the samples were digested using RNase H in the following reaction mixture at 37°C for 20 min: 2 μL sample, 0.5 μL 10× RNase H reaction buffer, 0.5 μL RNase H, and 2 μL H_2O. The digested samples were then mixed 1:1 (v/v) with formamide and run on a denaturing PAGE-urea gel in 1× TBE buffer at 60°C.

Statistics

All statistical analyses were performed using GraphPad Prism 8 Software. Significance was set at $\alpha = 0.05$. Comparisons between groups were assessed using one-way ANOVA.

SUPPLEMENTAL INFORMATION

Supplemental Information can be found online at https://doi.org/10.1016/j.omto.2020.07.013.

AUTHOR CONTRIBUTIONS

V.A., B.S.S., Y.T., and A.F. designed the experiments. V.A., B.S.S., Y.T., A.F., A.L., and A.A. conducted the experiments. V.A., B.S.S., Y.T., A.F., P.B., and A.A. analyzed the data. V.A., P.B., G.B., and R.A.D. helped put together the manuscript.

CONFLICTS OF INTEREST

The authors declare no competing interests.

ACKNOWLEDGMENTS

We would like to thank members of Jordan Miller's lab for providing the Nikon Eclipse Ti-E inverted fluorescent microscope, members of David Zhang's lab for providing feedback on the DNA-protected RNA designs of the ORAD system, and members of Rebekah Drezek's lab for editorial assistance. We would also like to thank the Baylor College of Medicine Medical Scientist Training Program (MSTP) for providing training support throughout the duration of the project.

This work was supported, in part, by the Cancer Prevention and Research Institute of Texas (RR140081 to G.B.).

REFERENCES

1. GBD 2015 Risk Factors Collaborators (2016). Global, regional, and national comparative risk assessment of 79 behavioural, environmental and occupational, and metabolic risks or clusters of risks, 1990-2015: a systematic analysis for the Global Burden of Disease Study 2015. Lancet *388*, 1659–1724.
2. Chari, R.V. (2008). Targeted cancer therapy: conferring specificity to cytotoxic drugs. Acc. Chem. Res. *41*, 98–107.
3. Beerenwinkel, N., Schwarz, R.F., Gerstung, M., and Markowetz, F. (2015). Cancer evolution: mathematical models and computational inference. Syst. Biol. *64*, e1–e25.
4. Frieder, R.E., Snow, S.G., Francis, M.S., and Brodsky, B.S. (2015). The evolution of multigene panel testing for hereditary cancers. Am. J. Obstet. Gynecol. *212*, 123.
5. Ross, J.S., and Cronin, M. (2011). Whole cancer genome sequencing by next-generation methods. Am. J. Clin. Pathol. *136*, 527–539.
6. SantaLucia, J., Jr., and Hicks, D. (2004). The thermodynamics of DNA structural motifs. Annu. Rev. Biophys. Biomol. Struct. *33*, 415–440.
7. Serra, M.J., and Turner, D.H. (1995). Predicting thermodynamic properties of RNA. Methods Enzymol. *259*, 242–261.
8. Sugimoto, N., Nakano, S., Katoh, M., Matsumura, A., Nakamuta, H., Ohmichi, T., Yoneyama, M., and Sasaki, M. (1995). Thermodynamic parameters to predict stability of RNA/DNA hybrid duplexes. Biochemistry *34*, 11211–11216.
9. Shu, D., Shu, Y., Haque, F., Abdelmawla, S., and Guo, P. (2011). Thermodynamically stable RNA three-way junction for constructing multifunctional nanoparticles for delivery of therapeutics. Nat. Nanotechnol. *6*, 658–667.
10. Piao, X., Wang, H., Binzel, D.W., and Guo, P. (2018). Assessment and comparison of thermal stability of phosphorothioate-DNA, DNA, RNA, 2′-F RNA, and LNA in the context of Phi29 pRNA 3WJ. RNA *24*, 67–76.
11. Zhang, D.Y., Chen, S.X., and Yin, P. (2012). Optimizing the specificity of nucleic acid hybridization. Nat. Chem. *4*, 208–214.
12. Manche, L., Green, S.R., Schmedt, C., and Mathews, M.B. (1992). Interactions between double-stranded RNA regulators and the protein kinase DAI. Mol. Cell. Biol. *12*, 5238–5248.
13. Kawai, T., and Akira, S. (2007). Antiviral signaling through pattern recognition receptors. J. Biochem. *141*, 137–145.
14. Hornung, V., Ellegast, J., Kim, S., Brzózka, K., Jung, A., Kato, H., Poeck, H., Akira, S., Conzelmann, K.K., Schlee, M., et al. (2006). 5′-Triphosphate RNA is the ligand for RIG-I. Science *314*, 994–997.
15. Kato, H., Sato, S., Yoneyama, M., Yamamoto, M., Uematsu, S., Matsui, K., Tsujimura, T., Takeda, K., Fujita, T., Takeuchi, O., and Akira, S. (2005). Cell type-specific involvement of RIG-I in antiviral response. Immunity *23*, 19–28.
16. Kato, H., Takeuchi, O., Sato, S., Yoneyama, M., Yamamoto, M., Matsui, K., Uematsu, S., Jung, A., Kawai, T., Ishii, K.J., et al. (2006). Differential roles of MDA5 and RIG-I helicases in the recognition of RNA viruses. Nature *441*, 101–105.
17. Kawai, T., Takahashi, K., Sato, S., Coban, C., Kumar, H., Kato, H., Ishii, K.J., Takeuchi, O., and Akira, S. (2005). IPS-1, an adaptor triggering RIG-I- and Mda5-mediated type I interferon induction. Nat. Immunol. *6*, 981–988.
18. Saha, S.K., Pietras, E.M., He, J.Q., Kang, J.R., Liu, S.Y., Oganesyan, G., Shahangian, A., Zarnegar, B., Shiba, T.L., Wang, Y., and Cheng, G. (2006). Regulation of antiviral responses by a direct and specific interaction between TRAF3 and Cardif. EMBO J. *25*, 3257–3263.
19. Pichlmair, A., Schulz, O., Tan, C.P., Näslund, T.I., Liljeström, P., Weber, F., and Reis e Sousa, C. (2006). RIG-I-mediated antiviral responses to single-stranded RNA bearing 5′-phosphates. Science *314*, 997–1001.
20. Takahashi, K., Kawai, T., Kumar, H., Sato, S., Yonehara, S., and Akira, S. (2006). Roles of caspase-8 and caspase-10 in innate immune responses to double-stranded RNA. J. Immunol. *176*, 4520–4524.
21. Yamamoto, M., Sato, S., Hemmi, H., Hoshino, K., Kaisho, T., Sanjo, H., Takeuchi, O., Sugiyama, M., Okabe, M., Takeda, K., and Akira, S. (2003). Role of adaptor TRIF in the MyD88-independent toll-like receptor signaling pathway. Science *301*, 640–643.
22. Buskiewicz, I.A., Koenig, A., Huber, S.A., and Budd, R.C. (2012). Caspase-8 and FLIP regulate RIG-I/MDA5-induced innate immune host responses to picornaviruses. Future Virol. *7*, 1221–1236.
23. Ghosh, S.K., Kusari, J., Bandyopadhyay, S.K., Samanta, H., Kumar, R., and Sen, G.C. (1991). Cloning, sequencing, and expression of two murine 2′-5′-oligoadenylate synthetases. Structure-function relationships. J. Biol. Chem. *266*, 15293–15299.
24. Díaz-Guerra, M., Rivas, C., and Esteban, M. (1997). Activation of the IFN-inducible enzyme RNase L causes apoptosis of animal cells. Virology *236*, 354–363.
25. Mitelman, F., Johansson, B., and Mertens, F. (2007). The impact of translocations and gene fusions on cancer causation. Nat. Rev. Cancer *7*, 233–245.
26. Nambiar, M., Kari, V., and Raghavan, S.C. (2008). Chromosomal translocations in cancer. Biochim. Biophys. Acta *1786*, 139–152.
27. Turc-Carel, C., Aurias, A., Mugneret, F., Lizard, S., Sidaner, I., Volk, C., Thiery, J.P., Olschwang, S., Philip, I., Berger, M.P., et al. (1988). Chromosomes in Ewing's sarcoma. I. An evaluation of 85 cases of remarkable consistency of t(11;22)(q24;q12). Cancer Genet. Cytogenet. *32*, 229–238.
28. Tsugita, M., Yamada, N., Noguchi, S., Yamada, K., Moritake, H., Shimizu, K., Akao, Y., and Ohno, T. (2013). Ewing sarcoma cells secrete EWS/Fli-1 fusion mRNA via microvesicles. PLoS ONE *8*, e77416.
29. Kato, H., Takeuchi, O., Mikamo-Satoh, E., Hirai, R., Kawai, T., Matsushita, K., Hiiragi, A., Dermody, T.S., Fujita, T., and Akira, S. (2008). Length-dependent recognition of double-stranded ribonucleic acids by retinoic acid-inducible gene-I and melanoma differentiation-associated gene 5. J. Exp. Med. *205*, 1601–1610.
30. Donovan, J., Whitney, G., Rath, S., and Korennykh, A. (2015). Structural mechanism of sensing long dsRNA via a noncatalytic domain in human oligoadenylate synthetase 3. Proc. Natl. Acad. Sci. USA *112*, 3949–3954.
31. Donovan, J., Dufner, M., and Korennykh, A. (2013). Structural basis for cytosolic double-stranded RNA surveillance by human oligoadenylate synthetase 1. Proc. Natl. Acad. Sci. USA *110*, 1652–1657.
32. Nallagatla, S.R., and Bevilacqua, P.C. (2008). Nucleoside modifications modulate activation of the protein kinase PKR in an RNA structure-specific manner. RNA *14*, 1201–1213.
33. Nallagatla, S.R., Toroney, R., and Bevilacqua, P.C. (2008). A brilliant disguise for self RNA: 5′-end and internal modifications of primary transcripts suppress elements of innate immunity. RNA Biol. *5*, 140–144.
34. Durbin, A.F., Wang, C., Marcotrigiano, J., and Gehrke, L. (2016). RNAs Containing Modified Nucleotides Fail To Trigger RIG-I Conformational Changes for Innate Immune Signaling. MBio *7*, e00833-16.
35. Łabno, A., Tomecki, R., and Dziembowski, A. (2016). Cytoplasmic RNA decay pathways - Enzymes and mechanisms. Biochim. Biophys. Acta *1863*, 3125–3147.
36. Houseley, J., and Tollervey, D. (2009). The many pathways of RNA degradation. Cell *136*, 763–776.
37. Matsukura, M., Shinozuka, K., Zon, G., Mitsuya, H., Reitz, M., Cohen, J.S., and Broder, S. (1987). Phosphorothioate analogs of oligodeoxynucleotides: inhibitors of replication and cytopathic effects of human immunodeficiency virus. Proc. Natl. Acad. Sci. USA *84*, 7706–7710.
38. Ono, T., Scalf, M., and Smith, L.M. (1997). 2′-Fluoro modified nucleic acids: polymerase-directed synthesis, properties and stability to analysis by matrix-assisted laser desorption/ionization mass spectrometry. Nucleic Acids Res. *25*, 4581–4588.
39. Sousa, R., and Padilla, R. (1995). A mutant T7 RNA polymerase as a DNA polymerase. EMBO J. *14*, 4609–4621.
40. Integrated DNA Technologies.. Chemical synthesis and purification of oligonucleotides. http://sfvideo.blob.core.windows.net/sitefinity/docs/default-source/technical-report/chemical-synthesis-of-oligos.pdf?sfvrsn=40483407_8.
41. Chiu, Y.H., Macmillan, J.B., and Chen, Z.J. (2009). RNA polymerase III detects cytosolic DNA and induces type I interferons through the RIG-I pathway. Cell *138*, 576–591.
42. Shir, A., and Levitzki, A. (2002). Inhibition of glioma growth by tumor-specific activation of double-stranded RNA-dependent protein kinase PKR. Nat. Biotechnol. *20*, 895–900.

43. Dirks, R.M., Ueda, C.T., and Pierce, N.A. (2013). Retraction. Proc. Natl. Acad. Sci. USA *110*, 384.

44. Bianchi, F., Pretto, S., Tagliabue, E., Balsari, A., and Sfondrini, L. (2017). Exploiting poly(I:C) to induce cancer cell apoptosis. Cancer Biol. Ther. *18*, 747–756.

45. Qu, J., Hou, Z., Han, Q., Zhang, C., Tian, Z., and Zhang, J. (2013). Poly(I:C) exhibits an anti-cancer effect in human gastric adenocarcinoma cells which is dependent on RLRs. Int. Immunopharmacol. *17*, 814–820.

46. Matsumoto, M., and Seya, T. (2008). TLR3: interferon induction by double-stranded RNA including poly(I:C). Adv. Drug Deliv. Rev. *60*, 805–812.

47. Zamore, P.D., Tuschl, T., Sharp, P.A., and Bartel, D.P. (2000). RNAi: double-stranded RNA directs the ATP-dependent cleavage of mRNA at 21 to 23 nucleotide intervals. Cell *101*, 25–33.

48. Cooper, G.M. (1992). Elements of Human Cancer (Jones and Bartlett Publishers).

49. Kailasan Vanaja, S., Rathinam, V.A., Atianand, M.K., Kalantari, P., Skehan, B., Fitzgerald, K.A., and Leong, J.M. (2014). Bacterial RNA:DNA hybrids are activators of the NLRP3 inflammasome. Proc. Natl. Acad. Sci. USA *111*, 7765–7770.

50. Martinon, F., Burns, K., and Tschopp, J. (2002). The inflammasome: a molecular platform triggering activation of inflammatory caspases and processing of proIL-beta. Mol. Cell *10*, 417–426.

51. Suspène, R., Renard, M., Henry, M., Guétard, D., Puyraimond-Zemmour, D., Billecocq, A., Bouloy, M., Tangy, F., Vartanian, J.P., and Wain-Hobson, S. (2008). Inversing the natural hydrogen bonding rule to selectively amplify GC-rich ADAR-edited RNAs. Nucleic Acids Res. *36*, e72.

52. Dieci, G., Fiorino, G., Castelnuovo, M., Teichmann, M., and Pagano, A. (2007). The expanding RNA polymerase III transcriptome. Trends Genet. *23*, 614–622.

53. Lemaire, P.A., Anderson, E., Lary, J., and Cole, J.L. (2008). Mechanism of PKR Activation by dsRNA. J. Mol. Biol. *381*, 351–360.

54. Nanduri, S., Carpick, B.W., Yang, Y., Williams, B.R., and Qin, J. (1998). Structure of the double-stranded RNA-binding domain of the protein kinase PKR reveals the molecular basis of its dsRNA-mediated activation. EMBO J. *17*, 5458–5465.

55. Reikine, S., Nguyen, J.B., and Modis, Y. (2014). Pattern Recognition and Signaling Mechanisms of RIG-I and MDA5. Front. Immunol. *5*, 342.

56. Kolakofsky, D., Kowalinski, E., and Cusack, S. (2012). A structure-based model of RIG-I activation. RNA *18*, 2118–2127.

57. Finn, O.J. (2012). Immuno-oncology: understanding the function and dysfunction of the immune system in cancer. Ann. Oncol. *23* (*Suppl 8*), viii6–viii9.

58. Mu, X., Greenwald, E., Ahmad, S., and Hur, S. (2018). An origin of the immunogenicity of in vitro transcribed RNA. Nucleic Acids Res. *46*, 5239–5249.

59. Asthana, V., Tang, Y., Ferguson, A., Bugga, P., Asthana, A., Evans, E.R., Chen, A.L., Stern, B.S., and Drezek, R.A. (2018). An inexpensive, customizable microscopy system for the automated quantification and characterization of multiple adherent cell types. PeerJ *6*, e4937.